VTT Technical Research Centre of Finland

Iodine release from high-burnup fuel structures: Separate-effect tests and simulated fuel pellets for better understanding of iodine behaviour in nuclear fuels

Heikinheimo, Janne; Kärkelä, Teemu; Tyrpekl, Václav; Niznanský, Matj; Gouëllo, Mélany; Tapper, Unto

Document Version
Publisher's final version

Link to publication

ORIGINAL PAPER

Iodine release from high-burnup fuel structures: Separate-effect tests and simulated fuel pellets for better understanding of iodine behaviour in nuclear fuels

Janne Heikinheimo[1] · Teemu Kärkelä[1] · Václav Tyrpekl[2] · Matěj Nižňanský[2,3] · Mélany Gouëllo[1] · Unto Tapper[1]

Abstract

Iodine release modelling of nuclear fuel pellets has major uncertainties that restrict applications in current fuel performance codes. The uncertainties origin from both the chemical behaviour of iodine in the fuel pellet and the release of different chemical species. The structure of nuclear fuel pellet evolves due to neutron and fission product irradiation, thermo-mechanical loads and fission product chemical interactions. This causes extra challenges for the fuel behaviour modelling. After sufficient amount of irradiation, a new type of structure starts forming at the cylindrical pellet outer edge. The porous structure is called high-burnup structure or rim structure. The effects of high-burnup structure on fuel behaviour become more pronounced with increasing burnup. As the phenomena in the nuclear fuel pellet are diverse, experiments with simulated fuel pellets can help in understanding and limiting the problem at hand. As fission gas or iodine release behaviour from high-burnup structure is not fully understood, the current preliminary study focuses on (i) sintering of porous fuel samples with Cs and I, (ii) measurements of released species during the annealing experiments and (iii) interpretation of the iodine release results with the scope of current fission gas release models.

Introduction

High release of iodine has been reported in the annealing experiments of irradiated fuels [1–3]. In the case of hyperstoichiometric UO_2, the release of iodine tends to surpass that of xenon [4]. The release of iodine should be reduced if it appears in the fuel in less volatile chemical state, such as CsI. However, earlier studies indicate that the formation of CsI in the fuel should be minor [4]. Despite of the results from international fission product (FP) release experiments at various temperatures [1–3] and mechanistic approaches for fission product transport in irradiated UO_2 [5], uncertainties exist for iodine chemical state in the fuel and its release.

SIMFUEL pellets containing volatile elements require a special approach to retain the volatile material inside the pellet during the sintering procedure. The volatile elements can be implanted in the sintered pellets with ion-implantation techniques [6] or alternative sintering approaches could be used for UO_2-CsI mixture [7, 8]. Typically, a very high temperature is required for UO_2 sintering (over 1700 °C) but the temperature can be reduced with the spark plasma sintering (SPS) method [8, 9]. Also, containers with reduced temperature and increased hold time have been successfully tried for the SIMFUEL sintering [7]. In the case of ion-implanted iodine, related iodine diffusion experiments have been conducted with thermal annealing [6].

Non-radioactive CeO_2 has been previously applied in fuel pellet-related experiments due to the same crystallographic structure and similar mechanical properties as UO_2 [10–13]. In this study, we applied CeO_2 powder as surrogate material for UO_2 and PuO_2. The CeO_2 powder was mixed with CsI powder and pressed into pellets with SPS method. Annealing experiments were performed for SPS pellets.

✉ Janne Heikinheimo
janne.heikinheimo@vtt.fi

1   Nuclear Energy, VTT Technical Research Centre of Finland Ltd, 02150 Espoo, Finland

2   Department of Inorganic Chemistry, Faculty of Science, Charles University, 128 00 Prague, Czech Republic

3   Department of Materials Engineering, Institute of Plasma Physics of the Czech Academy of Sciences, 182 00 Prague, Czech Republic

Experimental details

Sample preparation

The CeO_2 (Alfa Aesar 5 micron powder, 99.9%) and CsI (ACROS Organics, 99.999%) powders were mixed in desired ratio (1 mol% of CsI), blended and ground manually in a mortar. About 1.6 g of the powder mixture was poured into a graphite punch—die assembly (8 mm in diameter) and treated in SPS facility. The annealing was done in a SPS 10-4 10 Ton by Thermal Technology LLC (USA.). Maximum DC heating current is 4000 A at 10 V with 40 kW heating power. Temperature was measured on the die surface using a pyrometer with a measuring range of 600–2200 °C. The final sintering temperatures were set to 900, 1000 and 1100 °C bearing in mind that the allowed maximum sintering temperature is < 1200 °C due to the boiling point of CsI, which is about 1280 °C. The dwell time at the maximum sintering temperature was 5 minutes, while the applied pressure reached 80 MPa.

Final compact dimensions were measured using a micrometre screw KINEX 7031-02-025, and the corresponding geometrical density was calculated (linear approximation between CeO_2 and CsI). Phase composition of the samples was studied by X-ray powder diffraction (XRD) on a PANalytical X'Pert PRO diffractometer (CuKα radiation) and elaborated by Rietveld refinement using FullProf Suite.

The phase composition of the final compacts was confirmed by XRD and Rietveld fit, samples contained CeO_2 with fluorite structure (Fm-3m, $a = 5.41$ Å) and CsI (Pm-3m, $a = 4.57$ Å). The higher the sintering temperature, the higher was the observed density of the disc, crossing 81% of theoretical density at 1100 °C.

Experimental setup for release studies

The configuration of VTT's fission product transport facility used in the experiments is shown in Fig. 1. The facility has been applied previously, e.g. for the ruthenium transport studies in reactor coolant circuit [14]. The sample was heated to 1500 °C in an inert argon flow in order to produce vapour species. The total argon flow rate through the facility was 5.0 l/min (conditions 20 °C, 101.325 kPa, measured with a Thermal Mass Flowmeter TSI 3063, TSI Incorp.). The pressure inside the facility ranged from 102 to 104 kPa. The argon flow directed to the furnace tube was dry. The released species from CeO_2 + CsI sample were transported with gaseous atmosphere to particle analysers, a particle filter and liquid trap for iodine and caesium, respectively. Particle samples were also collected on holey carbon-coated copper (400 mesh) grids with the aspiration sampler. The collected particle samples were analysed with the Transmission Electron Microscopy (TEM). Dry air was applied for dilution of the sample flow for the aerosol analysers. The flow through the iodine trap was 4 l/min.

The liquid trap was filled with a solution of 0.1 M sodium hydroxide (NaOH) and was equipped with the Ion Selective Electrode (ISE) in order to monitor online the concentration of iodide. In addition, during the test, ten samplings (5 ml) were performed with a syringe in order to be analysed afterwards by Inductively Coupled Plasma Mass Spectrometry (ICP-MS). The analyses were performed with a Thermo Fisher Scientific HR-ICP-MS Element2 apparatus.
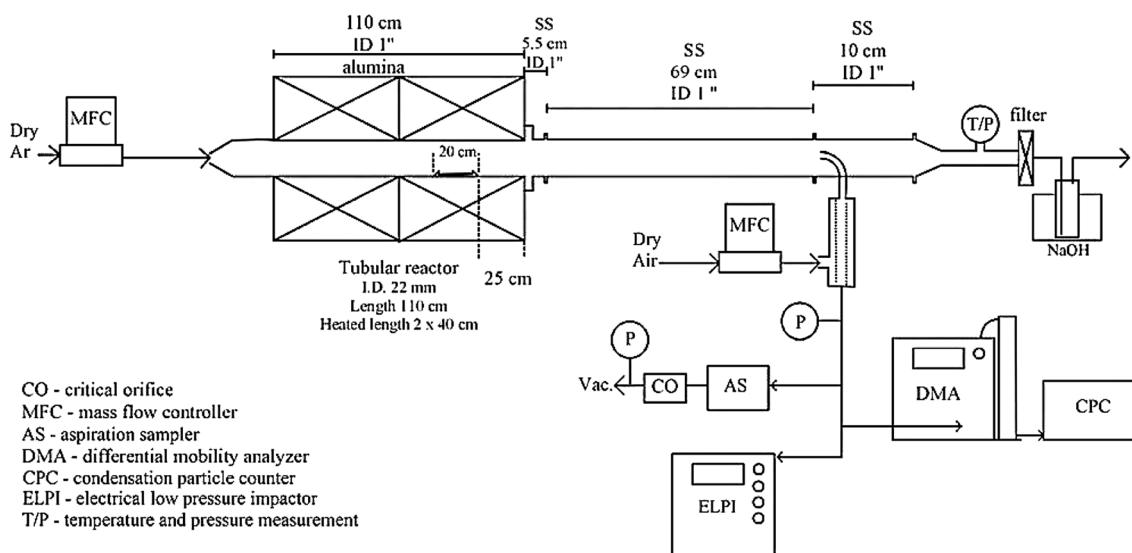
Fig. 1 Schematics of the experimental facility for the CeO_2 + CsI release and transport studies

For the ICP-MS, the iodine and caesium standards and controls, 0.5, 1, 10, 20 and 100 ppb, were diluted from the Reference Standard solutions (iodine: Inorganic Ventures CGICI1; caesium: Inorganic Ventures IV-STOCK-21). All measured solutions contained an internal standard; 10 μg/l of rhodium, to control the changes in signal. The samples were injected through PFA μflow nebulizer and double-pass spray chamber equipped with Peltier cooling unit. Washing time between the samples was 4 min with pump speed of 11 rpm.

The release experiments were started by placing a pellet sample into the reaction furnace and heating up the furnace to the set-point temperature (heating rate of 10 degrees per minute). The gas flow through the facility was started with the heating. When the furnace set-point was reached, the high-temperature (set-point) plateau was maintained for 60 min.

During the heat-up, plateau and cooling-down phases, the reaction products in the form of particles and gas were collected on filters and trapped in a 0.1 M sodium hydroxide solution. At the same time, iodine and particles in the gas phase were analysed with online devices. During the furnace heat-up and plateau phases, particle samples were collected from the gas flow on the TEM grid substrate for the analyses to be conducted later. After the experiment, the gas flows were stopped and the filter was removed. The crucible with the pellet sample was removed from the furnace the next day after the cooling down of furnace to room temperature.

Scanning electron microscopy

The pellets were analysed prior to the annealing experiments with the Scanning Electron Microscopy (SEM, Zeiss Crossbeam 540 equipped with EDAX Octane Elite^{TM} X-ray detector) to characterize pellet morphology and CsI distribution in the pellets. The imaging of the CeO_2 pellets were conducted using 4 kV electrons while the X-ray analysis was conducted using 15 kV electrons. The probe current was roughly 100 pA.

Results

Characterization of the samples and experimental procedure

The iodine release experiments were conducted with annealing of the sample pellets, similar to VERDON [2, 3] and HEVA [1] programmes and Turnbull et al.'s studies [15], with the difference that the object of study was a simulated fuel sample instead of irradiated fuel sample. The masses and theoretical densities of the pellets are indicated in Table 1. The table also shows sample outer surface-to-volume ratios. These values were graphically

calculated with the Matlab Image Viewer Distance tool for further comparison of the sample release behaviour as the sample pellets were partly cracked in the removal process from spark plasma sintering device.

Structural characterization of the samples

The studied samples were analysed in SEM to have an overview of the general morphology and degree of pellet porosity. The dispersion of CsI in pellets was studied using elemental analysis with EDS (energy-dispersive X-ray spectroscopy). Cross-section images verified that there are open cavities or pores between crystalline CeO_2 particles in all samples. The sintering was more complete with the higher sintering temperature.

Cs or I was not found on the sample cross-section surfaces in the EDS analyses as is indicated in Fig. 2a, b. However, when the CeO_2 pellet surface was analysed with SEM, all three samples showed several particles with bright contrast, c.f. Fig. 2c. According to EDS analyses, these particles were rich in caesium and iodine. Thus, it is possible to identify CsI on pellet surfaces based on the secondary electron images and conclude that CsI was typically found as particles at the grain boundaries. Being able to identify CsI by imaging is based on in-lens detector technique in Zeiss Gemini column for imaging secondary electrons (SE) at low electron energies. The in-lens detector is a high-contrast SE detector which is very sensitive, e.g. to charge conductivity of the specimen surface. In this case, it appears that CeO_2 has better charge conductivity leading to very bright contrast of CsI particles having poorer electron conductivity. The SPS-900 sample seemed to have more particles on the surface in comparison with SPS-1000 and SPS-1100, respectively.

### Iodine release and transport from the pellets

The release from the pellet sample in the crucible was determined by weighing the crucible with the pellet sample before and after each experiment. The difference in mass

Table 1 Experimental matrix of the CsI-doped CeO_2 samples containing sample mass and theoretical density

Sample sintering temperature (°C)	Sample mass (mg ± 1 mg)	Theoretical density (%)	Sample outer surface-to-volume ratio (1/cm)
900	1148	70	15.23
1000	1036	75	16.80
1100	1463	81	24.21

All samples had a similar doping concentration of 1 mol%. The outer surface-to-volume ratio has been measured for the samples as well

Fig. 2 SEM/EDS analysis of
the cross-sections surfaces of
the SPS-900 sample. In **b** and **d**
sum EDS spectrum comprise of
integrated X-ray counts per pix-
els in **a** and **c**. The labels in (**a**)
and (**c**), correspond to spot EDS
analyses but are not reproduced
here. The peak labels for iodine
(I), caesium (Cs) and cerium
(Ce) are to indicate their peak
locations
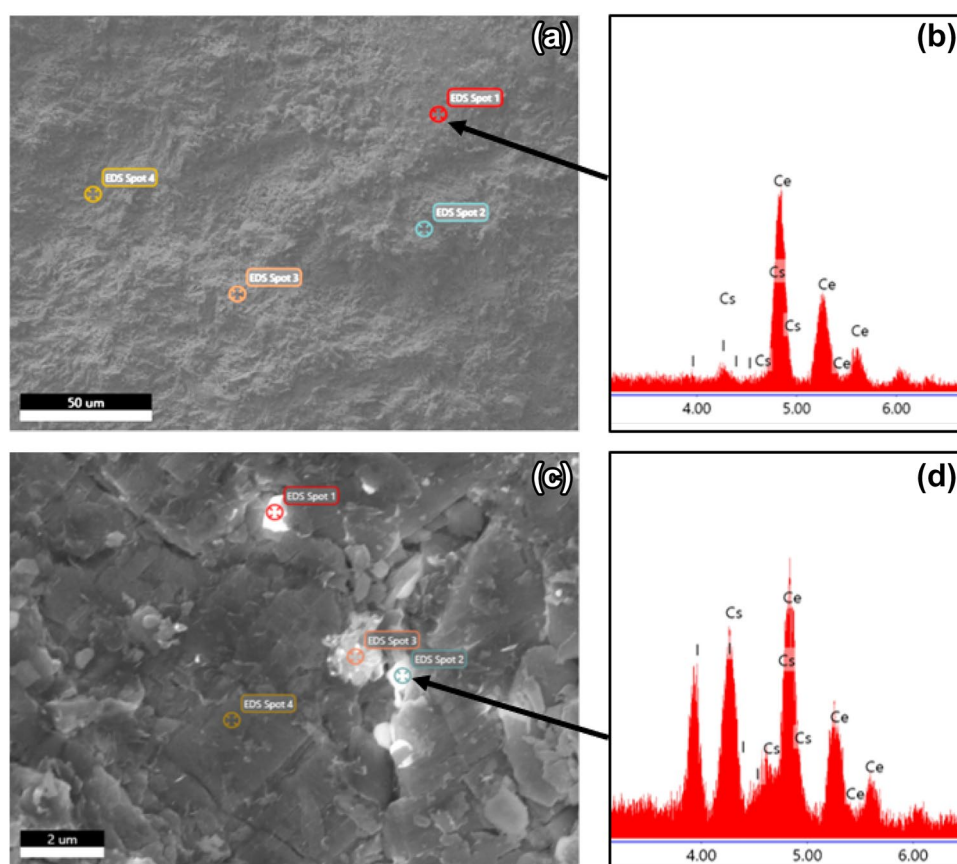
corresponds to the released mass. Similarly, the transported
mass to the filter was analysed by weighing the filter before
and after each experiment. The obtained results are pre-
sented in Table 2. Interestingly, the trend with the pellet
weight loss and filter weight gain contradicts with SPS-1000
sample indicating the release of different type or amount of
chemical species compared to the other samples. All pre-
annealed samples were grey in colour, typical for non-stoi-
chiometric CeO_2 with oxygen vacancies. After the annealing
experiments, the colour of all samples had changed to yellow
indicating the recovery of oxygen vacancies [16].

The NaOH trap measurements with ICP-MS show that
the release of iodine had already started at 650 °C. Around
1000–1100 °C, the release rate became faster. Then, from
1300 to 1500 °C, the release rate decreased for all the
samples.

Figure 3 shows the amount of iodine in the solution sam-
ples measured with ICP-MS. To compare the rate of released
iodine in relation to the sample microstructure, we normal-
ized the sample masses and macroscopic surface-to-volume
ratios by applying values in Table 1. The difference between
the SPS-900 and the other samples is notable. Based on the
mass measurements and following the analysis of particles
and filters, the iodine release for SPS-900 sample is close to

100% at the end of measurements. This has been indicated
with an axis for iodine fractional release in Fig. 3.

With the suitable selection of axes for the data in Fig. 3,
one can study the diffusional behaviour of the released
iodine. We applied an approach based on the Booth model
for fission gas release to have insight into iodine diffusional
behaviour [17, 18]. The analysis revealed that the release
behaviour of iodine was not purely dominated by diffusion
but also other phenomena were present. Possible additional
phenomena could be related to iodine chemical interactions
and tunnelling effect due to high concentration of iodine at
the grain boundaries. Detailed analysis on the iodine diffu-
sional behaviour is presented in the supplementary material.

In addition to the NaOH solution analysis with the HR-
ICP-MS, the particulate aerosol samples were analysed with
TEM and the filters set in front of the NaOH solution with
XRD. The analysis of the aerosol samples revealed that the
shape of the particles released from SPS-900 sample were
rounder in the shape. The XRD filter analysis revealed that
Cs was not released as CsO_2 compound from the SPS-900
sample. CsO_2 was present in the filters of SPS-1000 and
SPS-1100 sample annealing experiments. The amount of
Cs trapped in the filters was 9.9e-6, 9.3e-6 and 1.3e-5 mols
for SPS-900, SPS-1000 and SPS-1100 samples, respectively.
Negligible amount of Cs was found from the liquid trap after

Table 2 The release from the pellet sample in the crucible and the transported mass to the filter (values corresponding to the flow rate of 4 l/min through the filter)

Sample sintering temperature (°C)	Sample weight loss (mg ± 1 mg)	Filter weight gain (mg ± 0.1 mg)
900	27	6.88
1000	16	8.75
1100	18	3.75
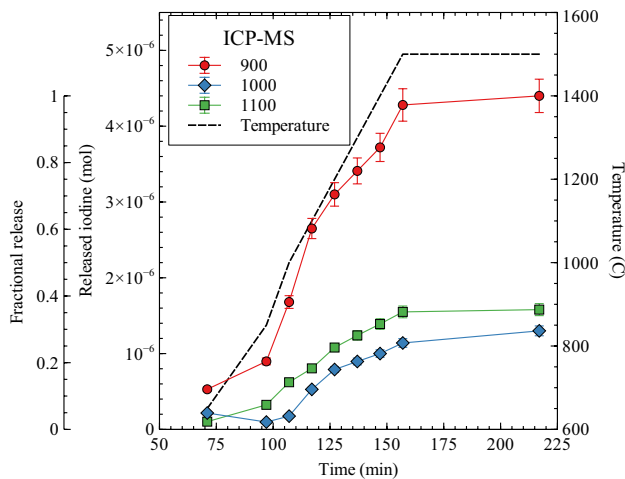
Fig. 3 Released iodine measured with the ICP-MS method with sample outer surface-to-volume ratio and mass normalized against the SPS-900 sample data. The complete fractional release of 1 is set for the SPS-900 series maximum

the filter. Further details are given in the supplementary material.

Conclusions

Sintering of the CeO_2 samples with 1 mol% of CsI was done at different temperatures and with similar pressure conditions reaching 80 MPa to create different porous structures and study their implications on caesium and iodine release. The concentrations of caesium and iodine correspond to above 60 MWd/kgU and 600 MWd/kgU burnups, respectively [4]. The theoretical densities of the samples annealed with 900 °C, 1000 °C and 1100 °C were 70%, 75% and 81%, respectively.

The release measurements were performed by annealing samples up to 1500 °C and measuring the trapped iodine and particles. Iodine was trapped in sodium hydroxide solution and particles were observed with particle analysers. In addition, some particle samples were analysed with TEM and particle filters with XRD. The sample sintered at 900 °C showed clearly different release behaviour in comparison with the other samples: the amount of released iodine was greater, and the filter analysis did not show caesium oxide as for the rest of the samples. The particle release behaviour, on the other hand, was similar between all samples. TEM analysis indicated that the released particles had more spherical shape for sample with 900 °C sintering in comparison to the other samples. Further data analysis of iodine release revealed that the behaviour may be dominated by other than simple grain boundary diffusion-related phenomena. Details in particle and further data analysis are documented in supplementary material.

The datasets generated during and/or analysed during the current study are available from the corresponding author on reasonable request.

References

1. J.-P. Leveque, B. Andre, G. Ducros, G.L. Marois, G. Lhiaubet, The HEVA experimental program. Nuclear Technol. **108**(1), 33–44 (1994). https://doi.org/10.13182/NT94-A35041

2. Y. Pontillon, S. Bernard, A. Gallais-Durning, B. Gleizes, E. Hanus, G. Ducros, Main outcomes relative to iodine behaviour from the VERDON/ISTP programme, in: International OECD/NEA-NUGENIA/SARNET Workshop on the Progress in Iodine Behaviour for NPP Accident Analysis and Management, Marseille, France (2020)

3. G. Ducros, Y. Pontillon, P.P. Malgouyres, Synthesis of the VERCORS experimental programme: separate-effect experiments on Fission Product release, in support of the PHEBUS-FP

programme. Ann. Nuclear Energy **61**, 75–87 (2013). https://doi.org/10.1016/j.anucene.2013.02.033

4. H. Kleykamp, The chemical state of the fission products in oxide fuels. J. Nuclear Mater. **131**, 221–246 (1985)

5. M.S. Veshchunov, V.D. Ozrin, V.E. Shestak, V.I. Tarasov, R. Dubourg, G. Nicaise, Development of the mechanistic code MFPR for modelling fission-product release from irradiated UO$_2$ fuel. Nuclear Eng. Des. **236**(2), 179–200 (2006). https://doi.org/10.1016/j.nucengdes.2005.08.006

6. M. Saidy, W.H. Hocking, J.F. Mouris, P. Garcia, G. Carlot, B. Pasquet, Thermal diffusion of iodine in UO$_2$ and UO$_{2+x}$. J. Nuclear Mater. **372**(2–3), 405–415 (2008). https://doi.org/10.1016/j.jnucmat.2007.03.272

7. J.Z. Liu, S. Miwa, K. Nakajima, M. Osaka, Synthesis of simulated fuels containing CsI under gas-tight condition. Nuclear Mater. Energy **26**, 100916 (2021). https://doi.org/10.1016/j.nme.2021.100916

8. T. Wangle, V. Tyrpekl, M. Cologna, J. Somers, Simulated UO$_2$ fuel containing CsI by spark plasma sintering. J. Nuclear Mater. **466**, 150–153 (2015). https://doi.org/10.1016/j.jnucmat.2015.07.030

9. V. Tyrpekl, M. Naji, M. Holzhäuser, D. Freis, D. Prieur, P. Martin, B. Cremer, M. Murray-Farthing, M. Cologna, On the role of the electrical field in spark plasma sintering of UO$_{2+x}$. Sci. Rep. **7**, 46625 (2017). https://doi.org/10.1038/srep46625

10. C. García-Ostos, J.A. Rodríguez-Ortiz, C. Arévalo, J. Cobos, F.J. Gotor, Y. Torres, Fabrication and characterization of CeO$_2$ pellets for simulation of nuclear fuel. Nuclear Eng. Des. **298**, 160–167 (2016). https://doi.org/10.1016/j.nucengdes.2015.12.026

11. C.A. Yablinsky, R. Devanathan, J. Pakarinen, J. Gan, D. Severin, C. Trautmann, T.R. Allen, Characterization of swift heavy ion irradiation damage in ceria. J. Mater. Res. **30**(9), 1473–1484 (2015). https://doi.org/10.1557/jmr.2015.43

12. J. Pakarinen, L. He, A.-R. Hassan, Y. Wang, M. Gupta, A. El-Azab, T.R. Allen, Annealing-induced lattice recovery in room-temperature xenon irradiated CeO$_2$: X-ray diffraction and electron energy loss spectroscopy experiments. J. Mater. Res. **30**(9), 1555–1562 (2015). https://doi.org/10.1557/jmr.2015.13

13. M. Khafizov, J. Pakarinen, L. He, D.H. Hurley, Impact of irradiation induced dislocation loops on thermal conductivity in ceramics. J. Am. Ceram. Soc. **102**(12), 7533–7542 (2019). https://doi.org/10.1111/jace.16616

14. T. Kärkelä, I. Kajan, U. Tapper, A. Auvinen, C. Ekberg, Ruthenium transport in an RCS with airborne CsI. Prog. Nuclear Energy **99**, 38–48 (2017). https://doi.org/10.1016/j.pnucene.2017.04.019

15. J. Turnbull, C. Friskney, J. Findlay, F. Johnson, A. Walter, The diffusion coefficients of gaseous and volatile species during the irradiation of uranium dioxide. J. Nuclear Mater. **107**(2), 168–184 (1982). https://doi.org/10.1016/0022-3115(82)90419-6

16. K. Ghillanyova, D. Galusek, Chapter 1: Ceramic oxides, in *Ceramics Science and Technology, Materials and Properties*, ed. By R. Riedel, I.-W. Chen, vol 2. Wiley (2011). ISBN 978-3-527-31156-9

17. A.H. Booth, A method of calculating fission gas diffusion from UO$_2$ fuel and its application to the X-2-f loop test, Technical Report CRDC-721, Atomic Energy of Canada Ltd. (496) (1957)

18. S. Kashibe, K. Une, Effect of additives (Cr$_2$O$_3$, Al$_2$O$_3$, SiO$_2$, MgO) on diffusional release of ^{133}Xe from UO$_2$ fuels. J. Nuclear Mater. **254**, 234–242 (1998)